GFD 2012 Lecture 3: Coherent Structures in 2D Fluid Dynamics and Structures in 3D Quasi-Geostrophic Fluid Dynamics

Jeffrey Weiss; notes by Rosalind Oglethorpe and Felicity Graham

June 20, 2012

1 Structure based scaling theory

In this lecture, we revisit the structure based temporal scaling theory for two-dimensional turbulent fluids. Scaling theory involves characterising the vortex population in terms of some of its properties; here, the total number of vortices N, vorticity ω, and vortex radius r are considered. The scaling behaviour of other vortex properties can be defined in terms of these quantities. We relate the three quantities to the scaling exponent ξ. Our assumptions from yesterday are that both energy and peak vorticity is conserved over the domain (note that this is only expected to be valid as $\mathrm{Re} \to \infty$), that all vorticity is contained within the vortices themselves, and that the probability distribution functions (PDFs) of the vortex properties evolve self-similarly. Note that the latter assumption implies that averages of powers of quantities scale the same as powers of averages, for example:

$$< r^n > (t) = c_n < r >^n (t), \tag{1}$$

where c_n is independent of time and $< . >$ denotes an averaged quantity.

1.1 Scaling of vortex properties

1.1.1 Circulation

Circulation Γ can be expressed in the following form

$$\Gamma_i = \int\limits_{vortex\ i} \omega \ \mathrm{d}^2\mathbf{x} \sim \omega_i r_i^2, \tag{2}$$

where constant relating Γ_i to $\omega_i r_i^2$ depends on the specific shape of the vortex. Hence, the evolution of the average circulation can be expressed as follows

$$< |\Gamma| > \sim < \omega >< r >^2 . \tag{3}$$

1.1.2 Energy

In 2D fluids, energy can be expressed in the following form

$$E = \frac{1}{2}\int |\mathbf{u}|^2 \mathrm{d}^2\mathbf{x} = \frac{1}{2}\int |\nabla\psi|^2 \mathrm{d}^2\mathbf{x}. \tag{4}$$

We integrate the above expression by parts, and since

$$\omega = \nabla^2\psi, \tag{5}$$

the energy can be expressed as

$$E = -\frac{1}{2}\int \omega\psi \mathrm{d}^2\mathbf{x}. \tag{6}$$

Here, we've assumed that either ψ goes to 0 at infinity, for an infinite domain, or that the domain has periodic boundaries.

By inverting $\omega = \nabla^2\psi$, the streamfunction becomes

$$\psi(\mathbf{x}) = \frac{1}{2\pi}\int \omega(\mathbf{x}')\ln|\mathbf{x}-\mathbf{x}'|\mathrm{d}^2\mathbf{x}'. \tag{7}$$

It is important to recognise that the vorticity generates the streamfunction; the streamfunction is not a locally derived property, but rather depends on the vorticity at near and far scales.

Substituting (7) into (6), we obtain

$$E = -\frac{1}{4\pi}\int \omega(\mathbf{x})\omega(\mathbf{x}')\ln|\mathbf{x}-\mathbf{x}'|\mathrm{d}^2\mathbf{x}\mathrm{d}^2\mathbf{x}'. \tag{8}$$

Now, considering isolated vortices, we sum over the domain to obtain

$$\begin{aligned} E &= -\frac{1}{4\pi}\Bigg[\sum_{i=1}^{N}\int_{vortex\ i} \omega(\mathbf{x})\omega(\mathbf{x}')\ln|\mathbf{x}-\mathbf{x}'|\ \mathrm{d}^2\mathbf{x}\mathrm{d}^2\mathbf{x}' \\ &\quad + \sum_{i\neq j}\int_{vortex\ i} \mathrm{d}^2\mathbf{x}\int_{vortex\ j} \omega(\mathbf{x})\omega(\mathbf{x}')\ln|\mathbf{x}-\mathbf{x}'|\ \mathrm{d}^2\mathbf{x}'\Bigg]. \end{aligned} \tag{9}$$

The first part of equation (9) describes the energy induced by self-interactions and the second part of the equation describes the energy induced by vortex-vortex interactions. The logarithmic term is the Green's function. For the purposes of scaling E, in what follows logarithmic corrections are ignored. Further details regarding the accuracy of this omission are discussed in [1].

From the interaction energy part of equation (9), it might be assumed that the energy of interaction scales like $N^2\Gamma^2$; however, this result disagrees with turbulence simulations [2]. To derive the scaling expression for E, we consider the numbers of same-sign and opposite-sign interactions between pairs of vortices from equation (9) above. The total vorticity is

zero so that we have an equal number of vortices with positive and negative vorticity (note that we assume that all vortices have approximately the same magnitude of vorticity)

$$\text{number of same-sign pairs} = 2\ \frac{N}{2}\left(\frac{N}{2}-1\right), \tag{10}$$

$$\text{number of opposite-sign pairs} = 2\ \left(\frac{N}{2}\right)^2. \tag{11}$$

It is clear that we get cancellation from the contribution of same-sign and opposite-sign pairs, so that E scales like the number of vortices rather than the number of pairs, i.e.

$$E_{\text{interaction}} \sim E_{\text{self}} \sim N < \Gamma >^2 . \tag{12}$$

This scaling now represents the combined effect of all vortices, rather than including them one at a time.

1.1.3 Enstrophy

The enstrophy equation can be expressed in the following form

$$Z = \frac{1}{2}\int |\omega|^2 \mathrm{d}^2\mathbf{x}, \tag{13}$$

from which, the scaling $Z \sim N < \omega >^2 < r >^2$ is obtained.

1.1.4 Final scalings

We have derived the scaling of Γ, E and Z as follows

$$< \Gamma > \sim < \omega >< r >^2, \tag{14}$$

$$E \sim N < \Gamma >^2, \tag{15}$$

$$Z \sim N < \omega >^2 < r >^2 . \tag{16}$$

Using these three quantities it is possible to express the scaling behaviour of the other vortex properties of the fluid field.

Now, our underlying assumptions that E and ω are conserved properties, namely

$$E \sim t^0, \text{ and} \tag{17}$$

$$< \omega > \sim t^0, \tag{18}$$

along with the evolution of the vortex number N observed in turbulence solutions

$$N(t) = N(T_0)\left(\frac{t}{t_0}\right)^{-\xi}, \tag{19}$$

provide the necessary closure to the theory. Empirically, we find that $N \sim t^{-\xi}$, where $\xi \sim 0.72$.

It is possible to express the time-evolution of all quantities in terms of scaling exponent ξ. For example,

$$E \sim t^0 \sim N < \Gamma >^2, \tag{20}$$

$$< \Gamma > \sim N^{-1/2} \sim t^{\xi/2}, \tag{21}$$

$$< r > \sim t^{\xi/4}. \tag{22}$$

Experimental studies have employed a range of numerical techniques to evaluate the evolution of vortex properties, as proposed by the scaling theory, and the value of the exponent ξ. These include direct numerical simulations (DNS) of 2D turbulence, point vortex models and laboratory experiments (e.g., that examine electrically excited vortices in a thin electrolyte). There is reasonable agreement between most experimental studies on the robustness of the scaling relationships and most studies estimate a value of ξ close to 0.7 [3, 4]. For example, Bracco et. al. [9] found good agreement between numerical simulations of decaying 2d turbulence and scaling theory for the vortex properties N, r, ω Γ and the scaling exponent ξ (figure 1). These agreements are relatively consistent between low and high resolution simulations (figure 2). However, some studies estimate slower or faster decays (table 1 from [3]). These differences may be due to the choice of analysis technique used, lateral dissipation and initial conditions such as the initial number of vortices (for example, all of the studies estimating a value of ξ much different to 0.7 had less than 100 vortices initially, which decreases the statistical significance of the results [3]). Whether experiments were run for a sufficient period of time to resolve the scaling regime has also been questioned [3]. Finally, despite reasonable agreement with experimental studies, there remains no convincing theory for the value of ξ.

2 Point-vortex model of 2D decaying turbulence

One of the primary goals of the point-vortex model was to construct the simplest model capturing the scaling regime of two-dimensional decaying turbulence [1]. In this model, 2D decaying turbulence is described by a "vortex gas" with circulations that determine the velocity field. Vortex same-sign merger is the dominant dissipative mechanism. The point-vortices are Hamiltonian, and hence, conservative, and each vortex has a position and circulation. Under this framework, same-sign pairs rotate without merger. However, given that when two point-vortices approach, the dissipation becomes important, we require a modification of the dynamics: when two same-sign vortices approach within a critical merger distance, they merge instantaneously, and are replaced by a single new vortex. The Hamiltonian dynamics then continues with this new vortex set. So, the new point-vortex dynamics is conservative everywhere in time except for a set of measure zero. This is a new class of dynamical system, which has been called punctuated Hamiltonian dynamics, and is neither conservative nor smoothly dissipative. This class of dynamical systems captures the intermittency of high Reynolds number turbulence.

2.1 Merger rules

When two same-sign vortices approach within a critical merger distance, determined to be less than approximately 3.3 times the vortex radius, the Hamiltonian dynamics are

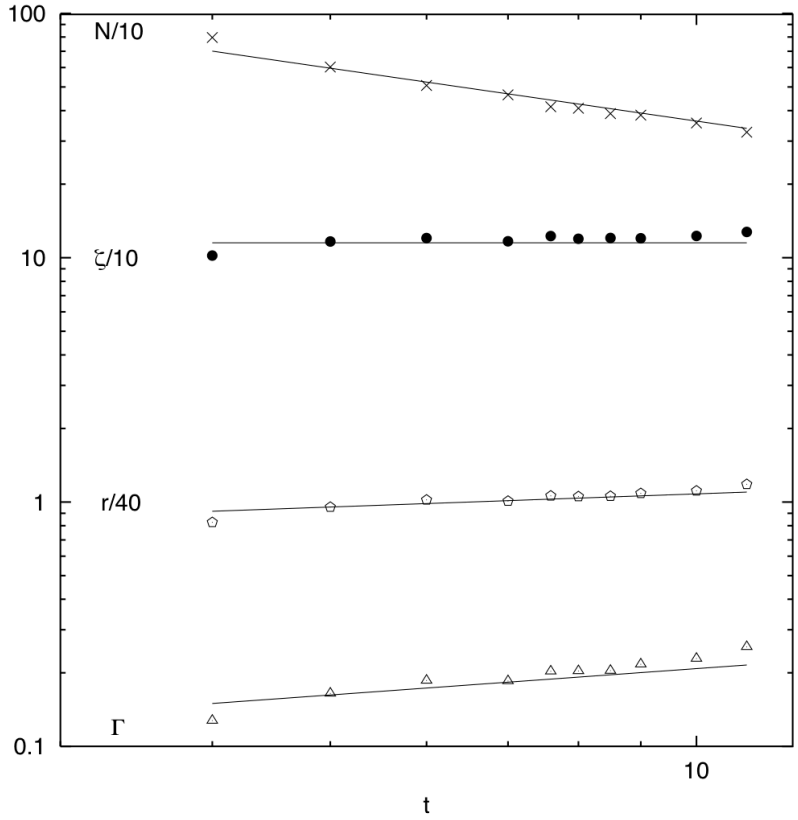

Figure 1: A comparison of average vortex number $N(t)$, vortex radius $r(t)$, vortex circulation magnitude $\Gamma(t)$, and peak vorticity ω (denoted by ζ in the figure) from a 2d decaying turbulence simulation (symbols) and scaling theory (solid lines) with $\xi = 0.72$. The model was of 4096^2 resolution. Each of the quantities has been multiplied by a suitable constant for graphical representation purposes. Note the logarithmic x- and y-axes. From [9].

interrupted and the two vortices merge into one new vortex. To capture this merger, we must modify our point-vortex model so that each vortex carries a dynamically inactive size. During the merger, the energy and peak vorticity are conserved, as in scaling theory. We further assume that the initial vortices have uniform peak vorticity, $\omega_i = \pm\omega_a$ for all i, and that the newly formed vortex also has the same vorticity (i.e. $\omega_{new} = \omega_1 = \omega_2$). Furthermore, we derive the following rules for the size and circulation of the new vortex based on the conservation of E

$$\Gamma_{new}^2 = \Gamma_1^2 + \Gamma_2^2, \tag{23}$$

$$r_{new}^4 = r_1^4 + r_2^4. \tag{24}$$

An interesting experiment would be to trace the linear momentum as two vortices merge. Since the circulation of the new vortex is not identical to the sum of the circulations of the

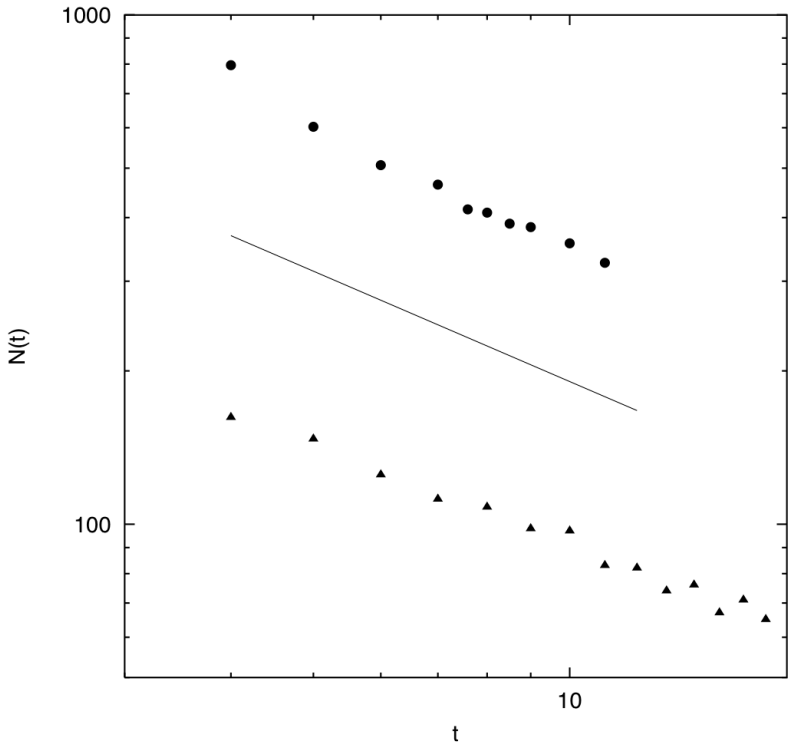

Figure 2: A comparison of average vortex number $N(t)$ estimated from decaying 2d turbulence simulations at high resolution (circles) and low resolution (triangles). Evolution predicted by scaling theory with $\xi = 0.72$ is represented by the solid line. Note the logarithmic x- and y-axes. From [9].

merging vortices, we would expect a change in linear momentum over the simulation.

2.2 Results of Punctuated model

Long integrations of the punctuated point-vortex model are obtained through renormalization, whereby the final state of an integration is used to initialise a new simulation with many more vortices, allowing us to reach the asymptotic scaling regime more quickly and to obtain sufficient data to reduce the sampling error. The model reproduces the vortex number N, vortex radius r_a, circulation magnitude Γ, enstrophy Z and kurtosis K_a predicted from scaling theory very well (figure 4). Figure 5 shows that the punctuated model produces scaled distributions that, within sampling variability, are constant in time and hence evolve self-similarly, although the model contains a higher number of small vortices than the turbulence solution.

3 Forced 2D turbulence

Forcing can be included in the 2D Navier-Stokes equations as follows

TABLE I. 2D turbulence experiments in which the vortex density decay rate was determined. The type of experiment is listed, as is an estimate of the initial number of vortices and the density decay exponent, χ. The second estimate from Bracco *et al.* (Ref. 17) (in parentheses) is for a subset of "strong" vortices.

Authors	Type	N_0	χ
McWilliams, 1990[a]	DNS	500	0.71
Tabeling *et al.*, 1991[b]	Lab	36–100	0.7 ± 0.1
Benzi *et al.*, 1992[c]	Pt. vortex	300	0.6 ± 0.05
Weiss and McWilliams, 1993[d]	Pt. vortex	400	0.72 ± 0.02
Cardoso *et al.*, 1994[e]	Lab	50	0.44 ± 0.1
Hansen *et al.*, 1998[f]	Lab	64	0.7 ± 0.1
Bracco *et al.*, 2000[g]	DNS	800	0.76 ± 0.03 (0.67 ± 0.02)
Trizac, 1998[h]	Molecular	50000	0.71 ± 0.01
Clercx and Nielsen, 2000[i]	DNS	100	1.0 ± 0.1
Sire and Chavanis, 2000[j]	Pt. vortex	50	1
Clercx *et al.*, 2003[k]	Lab./DNS	100	0.7 ± 0.1
van Bokhoven *et al.*, 2007[l]	DNS	64	0.63–0.93

Figure 3: table from [3]

$$\partial_t \mathbf{u} + \mathbf{u} \cdot \nabla \mathbf{u} = -\nabla p + \nu \nabla^2 \mathbf{u} - \alpha \mathbf{u} + \mathbf{f}, \tag{25}$$

where ∂_t denotes a partial derivative with respect to time, $\mathbf{u}$ is the 2D fluid velocity, p is pressure, ν is the viscosity, α is a linear frictional damping term and $\mathbf{f}$ is the forcing term [5]. The evolution of fluid properties (e.g. energy, enstrophy, vorticity) depends on the details of the forcing. The forced state produces an inverse energy cascade to larger scales, which arises primarily from the interaction of strain and vortices of different sizes, without requiring vortex merger or growth as in the non-forced simulations [5]. Forced 2D turbulence also produces a direct enstrophy cascade to smaller scales. We direct readers to [5] for a more comprehensive review of forced 2D turbulence.

4 Summary of 2D

We have considered the properties and evolution of coherent structures under decaying and forced 2D turbulence. 2D vortex dynamics can be modelled by both point vortices and elliptical vortices, where decaying turbulence acts like a "vortex gas". By implementing structure based scaling theory, we can represent all vortex properties in terms of a few quantities, such as vortex number N, vortex radius r and vorticity ω. Furthermore, the time-evolution of all vortex properties can be expressed in terms of the vortex exponent ξ. Numerical and experimental studies show a reasonable agreement of values of the exponent; disagreements on the value of ξ can be attributed to different lateral dissipations or initial conditions. The punctuated point vortex model is a Hamiltonian point vortex model that

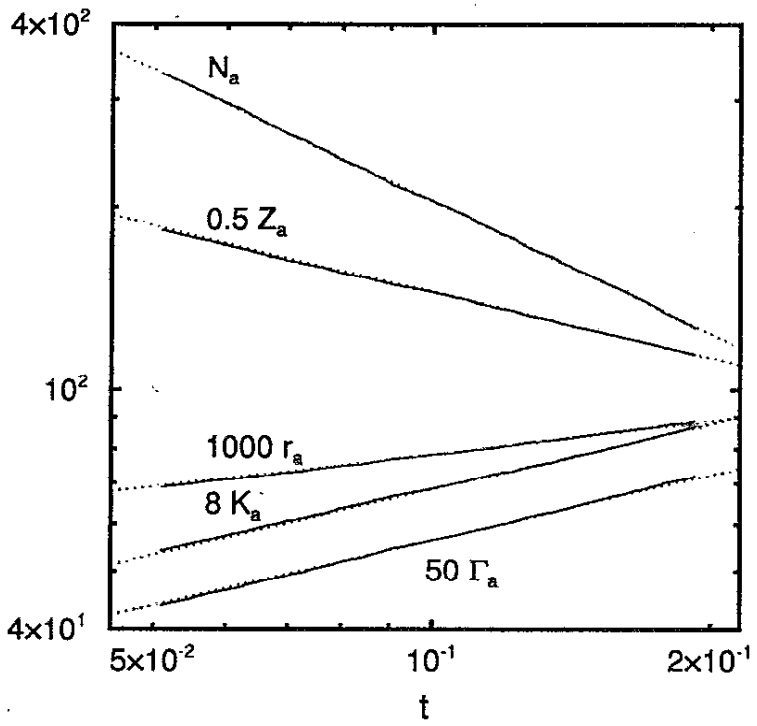

Figure 4: A comparison of average vortex number $N_a(t)$, vortex radius $r_a(t)$, vortex circulation magnitude $\Gamma_a(t)$, enstrophy $Z_a(t)$, and kurtosis $K_a(t)$ from the modified point-vortex model (solid lines) and scaling theory (dotted lines). In the model, $t_0 \leq t \leq t_0 + t'_{\rm end}$, where $t_0 = 0.050$ and $t'_{\rm end} \approx 0.14$ is the earliest time for one of the 30 cycles to reach $N = 100$. From [1].

has been modified such that vortices carry a size that is dynamically-inactive except during close approaches, when dissipative vortex merger occurs. This modified model captures the main features of 2D decaying turbulence well. According to [4],

> Concerning the decay problem, we are thus left at the present time with an elegant phenomenological theory ("universal decay theory"), which turns out to represent consistent sets of numerical and experimental observations.

However, there remains disagreement, particularly observable at Walsh Cottage, whether decay theory is truly "universal" and whether the numerical and experimental observations that underlie the theory are truly "consistent". Finally, it is possible to observe inverse energy cascades in forced 2D turbulence, although the properties and evolution of the coherent structures in this framework will depend on the mechanism of forcing.

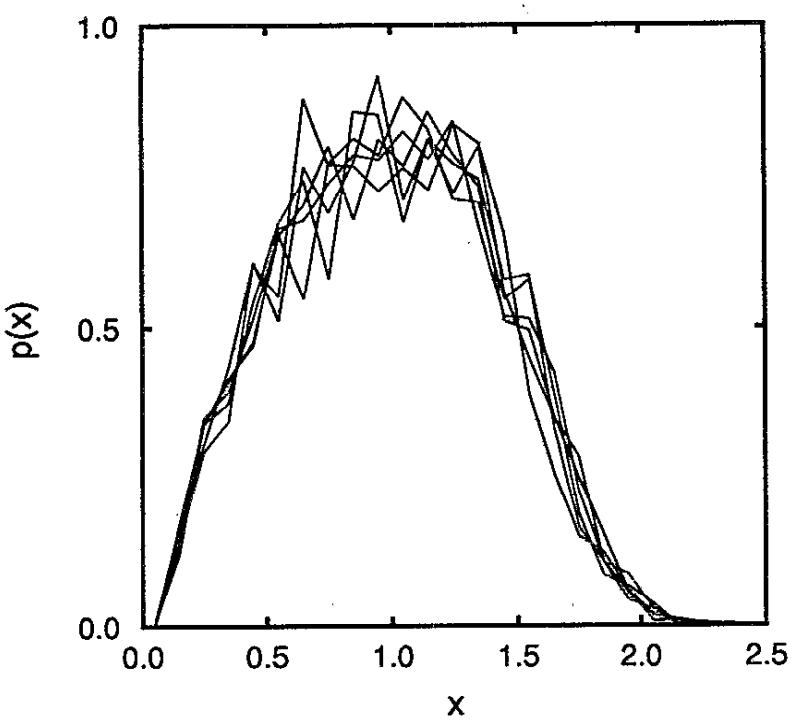

Figure 5: Probability distribution functions $p(x)$ at six different times from the punctuated point-vortex model calculated by averaging over 30 cycles. From [1].

5 Structures in 3D Quasigeostrophic Fluid Dynamics

5.1 Quasigeostrophic equations

We relax the 2D assumption and again consider the case of $Ro \ll 1$ (rapid rotation, i.e. scales slower than a day) and $F \ll 1$ (strong stratification). We assume the system is hydrostatic,

$$\frac{\partial p}{\partial z} + \rho g = 0, \tag{26}$$

so vertical gravity is balanced by the vertical pressure gradient, and that the fluid is thin, so the vertical dimension is much smaller than the horizontal dimensions. The 3D momentum equation is

$$\frac{\partial \mathbf{u}}{\partial t} + (\mathbf{u} \cdot \nabla)\mathbf{u} = -\nabla p + \nu \nabla^2 \mathbf{u} - \mathbf{f} \times \mathbf{u}, \tag{27}$$

and the fluid is incompressible

$$\nabla \cdot \mathbf{u} = 0. \tag{28}$$

The equation for conservation of mass is

$$\frac{\partial \rho}{\partial t} + (\mathbf{u} \cdot \nabla)\rho = 0, \tag{29}$$

and the vertical density gradient is given by

$$\frac{\partial \rho}{\partial z} = -\frac{N^2}{g}, \tag{30}$$

where $N = N(z)$ is the buoyancy frequency, which we assume to be horizontally uniform. An asymptotic analysis of the 3D equations, with $Ro \ll 1$, results in the quasigeostrophic equations.

At lowest order in Ro, we obtain

$$0 = -\nabla p - \mathbf{f} \times \mathbf{u}, \tag{31}$$

where the leading order velocity field is

$$\mathbf{u}(x, y, z, t) = (u, v, 0), \tag{32}$$

and $\mathbf{f}$ is the Coriolis parameter defined in lecture 1. Therefore, to leading order, the Coriolis force balances the horizontal pressure gradient. This is called geostrophy. The leading order velocity field is called the geostrophic velocity. The geostrophic velocity is 2D, so using incompressibility we can write the geostrophic velocity in terms of a streamfunction ψ:

$$(u, v) = \left(-\frac{\partial \psi}{\partial y}, \frac{\partial \psi}{\partial x} \right). \tag{33}$$

The next order in the asymptotic analysis gives the time dependence of $\mathbf{u}$ and the vertical velocity. Taking the curl of the next order of the momentum equation (27) and using incompressibility gives

$$\frac{D\omega}{Dt} - f\frac{\partial w}{\partial z} = \nu \nabla^2 \omega, \tag{34}$$

where we define the material derivative as

$$\frac{D}{Dt} \equiv \frac{\partial}{\partial t} + \mathbf{u} \cdot \nabla. \tag{35}$$

Using (29) and (30) we find an equation for the vertical velocity

$$w = -\frac{f}{N^2}\frac{D}{Dt}\frac{\partial \psi}{\partial z}. \tag{36}$$

We then combine this with (34) to obtain

$$\frac{D}{Dt}\left(\omega + \frac{\partial}{\partial z}\left(\frac{f^2}{N^2}\frac{\partial \psi}{\partial z} \right) \right) = \nu \nabla^2 \omega, \tag{37}$$

or

$$\frac{Dq}{Dt} = \nu \nabla^2 q, \tag{38}$$

to leading order, where q is the potential vorticity

$$q = \omega + \frac{\partial}{\partial z}\left(\frac{f^2}{N^2}\frac{\partial \psi}{\partial z} \right). \tag{39}$$

The first term in this equation is the relative vorticity obtained from the curl of the geostrophic velocity, $\omega = \nabla \times \mathbf{u} = \nabla^2_{2D}\psi$, and the second is the 'stretching term'. The vertical velocity causes stretching, which causes ω to change over time.

If N is constant, $N \neq N(z)$, then let $z' = Nz/f$, and the potential vorticity is given by the isotropic 3D Laplacian,

$$q = \nabla^2_{3D}\psi. \tag{40}$$

Equations (38) and (40) are the 3D quasigeostrophic (QG) equations for constant N. The 3D Laplacian in (40) indicates that the velocity field depends on the global 3D vorticity distribution.

We can compare the 3D QG equations with constant N to the 2D equations found previously:

	2D	3D QG, constant N
Inviscid vorticity equation:	$\frac{D\omega}{Dt} = 0$	$\frac{Dq}{Dt} = 0$
$q - \psi$ relationship:	$\omega = \nabla^2_{2D}\psi$	$q = \nabla^2_{3D'}\psi$

The similarity of the QG equations to the 2D vorticity equations leads to the same turbulent cascade theory as 2D. If $\nu = 0$, the potential vorticity q is invariant, so as in 2D there is no stretching of potential vorticity in QG. The energy

$$E = -\frac{1}{2}\int q(x)\psi(x)\mathrm{d}^3\mathbf{x} \tag{41}$$

is conserved, as in 2D, although there is now a contribution from potential energy. Thus the analysis of the 2D equations gives some insight into a fully 3D, asymptotic ($Ro \ll 1$, $F \ll 1$) regime.

5.2 QG decaying turbulence

Isotropy of the $q - \psi$ relation ($q = \nabla^2\psi$) and Taylor-Proudman ideas led to predictions of 3D isotropic spectra [7] and vertical barotropic (depth-independent) columns. However, numerical simulations (320^3 resolution) by [6] with random homogeneous and isotropic initial conditions show otherwise. The simulations use the dynamical QG equation

$$\frac{Dq}{Dt} = -\mathcal{D}, \tag{42}$$

with q defined in (39). The dissipation operator $\mathcal{D} = \nu\nabla^4 q$ represents the effects of the smaller scales of motion (ν is a small hyperviscosity). Figure 6 shows results of the simulations at four different times. The simulations show the formation of roughly spherical vortices (in stretched coordinates $z' = Nz/f$). The vortices are advected by the velocity field caused by the other vortices. The two primary interaction mechanisms that transform the vortex population are between same sign vortices: nearly horizontal merger, as we have already seen in 2D, and vertical vortex alignment, which is a new phenomenon to QG. Unlike vortex merger, the vertical alignment process is at least partly reversible (in that aligned vortices can move out of alignment) and the vortices remain distinct. The number

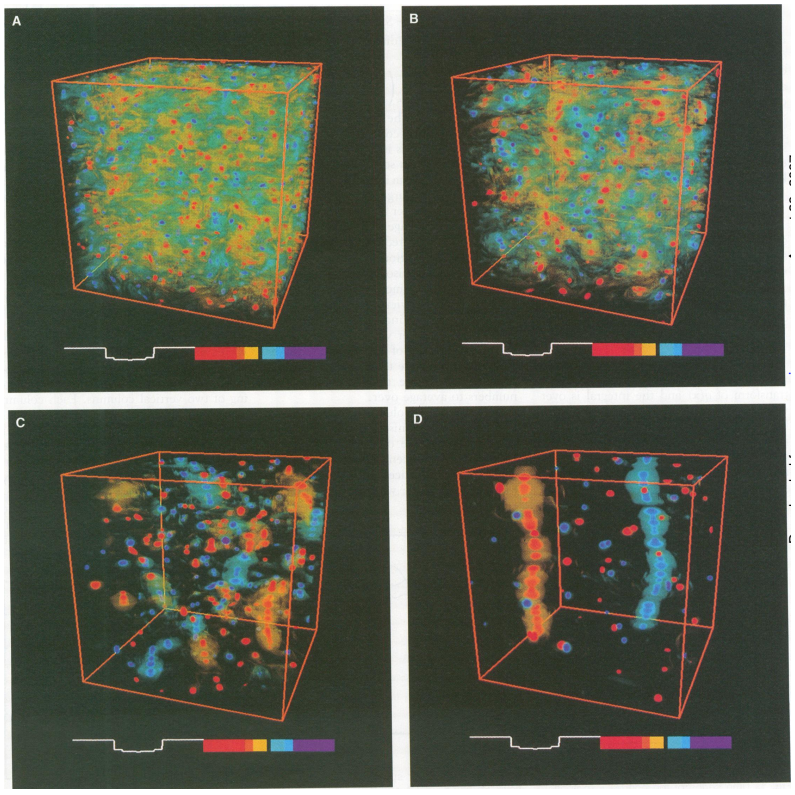

Figure 6: Potential vorticity $q(x, y, z')$ at (A) $t = 5.0$, (B) $t = 10.0$, (C) $t = 25.6$, and (D) $t = 72.1$. Taken from [6].

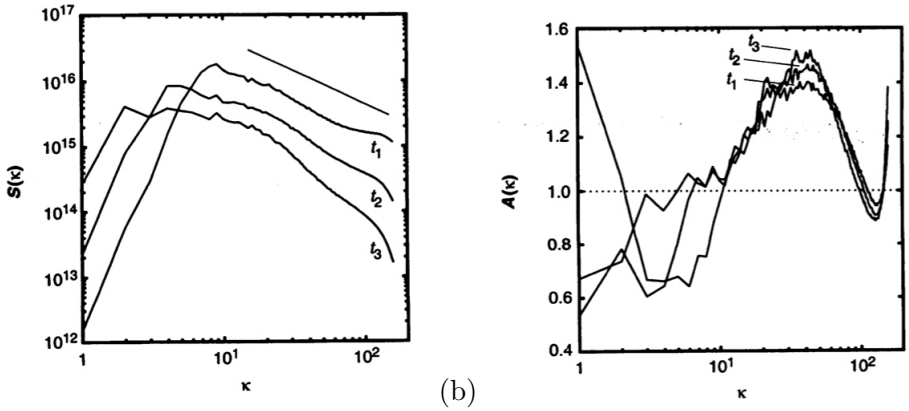

(a) (b)

Figure 7: (a) Wavenumber spectra of potential vorticity $S(\kappa)$ at $t_1 = 2.2$, $t_2 = 5.0$, and $t_3 = 10.0$. (b) Spectrum anisotropy $A(\kappa)$ at t_1, t_2, and t_3. Taken from [6].

of vortices decreases with time due to vortex merger, and the end result is of two columns of vertically aligned same-sign vortices, with the appearance of 'beads on a string'. This two column system is an analogue of the final vortex dipole in 2D. Similarly to 2D, the spectra are steeper than cascade theory predicts. In addition, there is significant spectral anisotropy,

$$A(\kappa) = \frac{3S_{z'}(\kappa)}{S_x(\kappa) + S_y(\kappa) + S_{z'}(\kappa)} \neq 1, \tag{43}$$

where $S_i(\kappa)$ are the directionally weighted wavenumber spectra of q

$$S_i(\kappa) = \int_{|\boldsymbol{\kappa}|=\kappa} \left(\frac{\kappa_i}{\kappa}\right)^2 |\hat{q}|^2 \mathrm{d}\boldsymbol{\kappa}, \tag{44}$$

$i = x, y, z'$, $\hat{q}(\boldsymbol{\kappa})$ is the 3D Fourier transform of $q(\mathbf{x})$, and $\kappa = |\boldsymbol{\kappa}|$ is the magnitude of the 3D wavenumber. Note that $\sum_i S_i = S(\kappa)$ which is the spectrum of $\hat{q}$ averaged over a shell of constant κ. Graphs of $S(\kappa)$ and $A(\kappa)$ are shown in figure 7. $A(\kappa) \neq 1$ indicates an anisotropic potential vorticity distribution at wave number κ. Due to this anisotropy (which is perhaps not surprising since D/Dt is not isotropic), the vortices are broader in the horizontal than the vertical.

5.3 QG vortex census ([8])

With the idea that 'geostrophic turbulence is controlled by the self-, pair-, and collective-dynamics of its coherent vortices', [8] did a vortex based statistical analysis of the results from the numerical simulations described above. This describes the structure and evolution of the vortex population in QG turbulence. A subjective automated algorithm is used to perform a vortex census to identify vortices and to measure their size, strength and shape. The result of this census is that the number of vortices decreases over time, which is expected from vortex merger. The mean enstrophy and mean circulation both increase over time. The mean of the peak vorticity, q_p, is approximately constant after an initial time (when the number of weak vortices appears to decrease faster than the number of strong

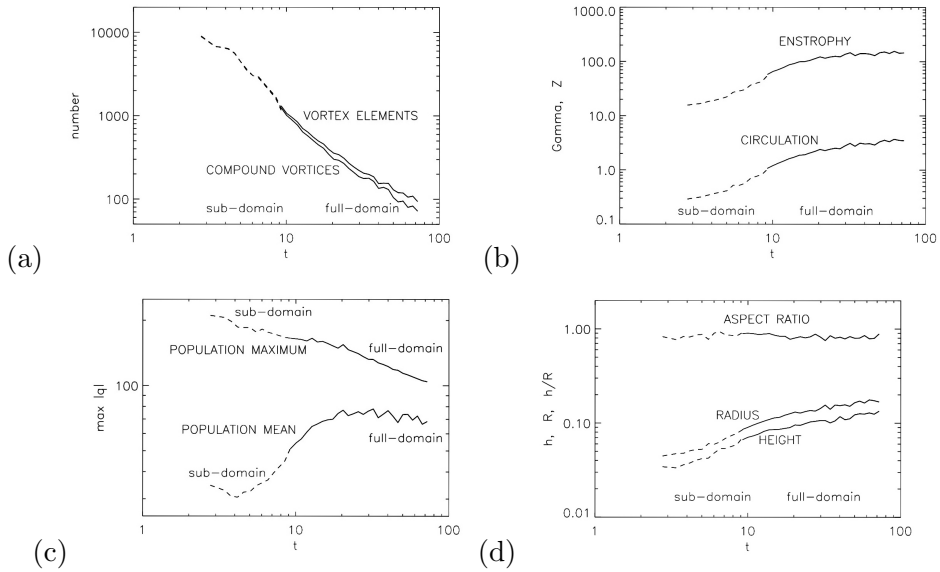

Figure 8: Graphs of the QG vortex census results: (a) number of vortices; (b) Γ and Z; (c) maximum of q_p and mean of q_p; (d) height h, radius R and aspect ratio. Taken from [8])

vortices), while the maximum of q_p decreases due to dissipative effects. The mean radius and height both increase over time, but the aspect ratio remains approximately constant (≈ 0.8). However, this constancy is not yet well understood. All these quantities appear to be described relatively well by power laws in t (see figure 8), which indicates the possibility of a scaling theory. Since there are no vertical velocity dynamics in the potential vorticity q, which is only advected horizontally, a scaling theory for QG can be derived in a similar way to the 2D scaling theory above.

5.4 QG scaling theory

The scaling theory is derived similarly to 2D (see section 1), with an additional empirical constant of the vortex aspect ratio. The assumptions are

- $q_p \sim$ constant
- Aspect ratio $\sim$ constant
- $N \sim t^{-\xi}$
- E conserved
- All vorticity is within vortices (this assumption turns out to be less valid than in 2D, because there are more background vorticity effects)

Following the same arguments as in the 2D scaling, we find scaling exponents for the different quantities in terms of a single exponent ξ. Empirically, from the results of the vortex census, $\xi \approx 1.25$, which is higher than for 2D. Therefore the number of coherent

vortices decreases more rapidly in 3D QG than in 2D. The assumption of constant aspect ratio gives

$$< h > \sim < R >, \tag{45}$$

where $< h >$ is the average vortex height and $< R >$ is the average vortex radius. Similarly to 2D, the circulation and enstrophy scale as

$$< \Gamma > \sim < q >< R >^2, \quad < Z > \sim < q >^2 < R >^2, \tag{46}$$

where q is potential vorticity (39). The energy is given by

$$E \sim \int \mathrm{d}^3\mathbf{x} \int \mathrm{d}^3\mathbf{x}' q(\mathbf{x}) q(\mathbf{x}') G(\mathbf{x}, \mathbf{x}'), \tag{47}$$

where G is a Green's function. In 2D, the Green's function $\sim \ln|\mathbf{x} - \mathbf{x}'|$, and we ignored the log terms in the scaling theory (see section 1.1.2). However, in 3D QG, the Green's function $\sim 1/|\mathbf{x} - \mathbf{x}'|$, so we must pick a length scale $L \sim |\mathbf{x} - \mathbf{x}'|$. This introduces some ambiguity. Considering the interaction energy between vortices, we choose $L \sim N^{-1/3}$, which is the typical vortex pair separation distance. This gives scalings of

$$< R > \sim < h > \sim t^{2\xi/9} = t^{0.28}, \tag{48}$$

$$< \Gamma > \sim < Z > \sim t^{4\xi/9} = t^{0.55}. \tag{49}$$

Considering the self-interaction energy, we choose $L \sim R$, which is the vortex size. This gives scalings of

$$< R > \sim < h > \sim t^{\xi/5} = t^{0.25}, \tag{50}$$

$$< \Gamma > \sim < Z > \sim t^{2\xi/5} = t^{0.50}. \tag{51}$$

For both choices of L, the scalings of $< R >$, $< h >$ and $< \Gamma >$ agree well with the vortex census results ($< R > \sim t^{0.29\pm0.05}$, $< h > \sim t^{0.28\pm0.05}$, $< \Gamma > \sim t^{0.45\pm0.10}$). There is more discrepancy in the exponent of $< Z >$, which is smaller in the vortex census results ($< Z > \sim t^{0.34\pm0.10}$) than in the scaling theory. This indicates that there is greater dissipation of vorticity q within the vortices in the numerical simulation than assumed in the scaling theory.

5.4.1 QG column waves

Another interesting observation from the numerical simulations in [6] is the appearance of vertical helical and planar waves on the vortex columns. These are shown in figure 9, but have not yet been studied.

References

[1] Weiss, J.B., McWilliams J.C. 1993. Temporal scaling behavior of decaying two-dimensional turbulence. *Phys. Fluids A*, 5(3), 608-621.

(a) 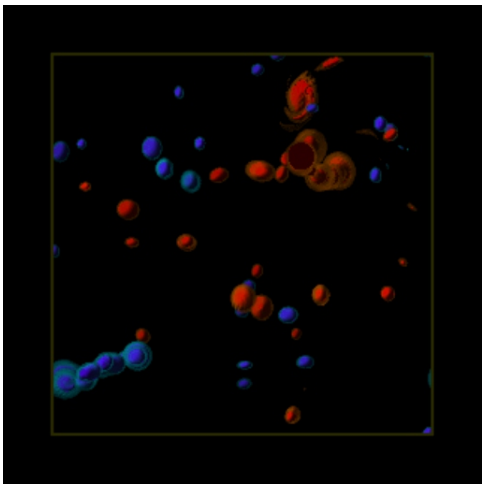 (b) 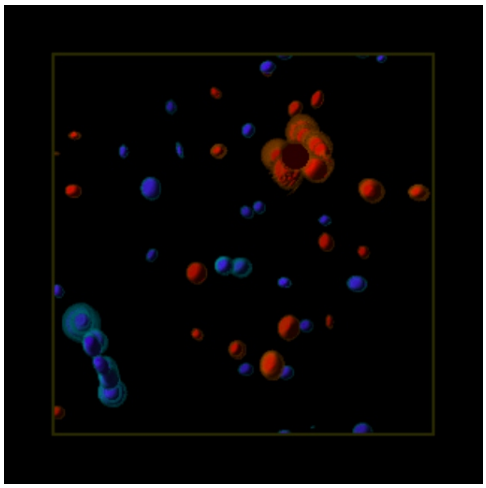

Figure 9: Top view of the simulation results [6] at two different times, showing a planar wave (blue vortex column, positive vorticity) and a helical wave (red vortex column, negative vorticity).

[2] Carnevale, G.F., McWilliams, J.C., Pomeau, Y., Weiss, J.B., Young, W.R. 1991. Evolution of vortex statistics in two-dimensional turbulence. *Phys. Rev. Lett,*, 6(21), 2735-2737.

[3] LaCasce, J.H. 2008. The vortex merger rate in freely decaying, two-dimensional turbulence. *Phys. Fluids*, 20, DOI: 10.1063/1.2957020.

[4] Tabeling P. 2002. Two-dimensional turbulence: a physicit approach. *Phys. Rep.*, 362, 1-62.

[5] Boffetta, G., Ecke, R.E. 2012. Two-dimensional turbulence. *Annu. Rev. Fluid Mech.*, 427-451, DOI:10.1146/annurev-fluid-120710-101240.

[6] McWilliams, J. C., Weiss, J. B., Yavney, I., 1994. Anisotropy and Coherent Vortex Structures in Planetary Turbulence. *Science*, 264, 410-413.

[7] Charney, J. G. 1971. Geostrophic Turbulence. *J. Atm. Sci.*, 28, 1087-1095.

[8] McWilliams, J. C., Weiss, J. B., Yavneh, I. 1999. The vortices of homogeneous geostrophic turbulence. *J. Fluid Mech.*, 401, 1-26.

[9] Bracco, A., McWilliams, J.C., Giuseppe, M., Provenzale, A., Weiss, J.B. 2000. Revisiting 2D Turbulence at Millenial Resolution, *Physics of Fluids*, 12, 2931-2941.